

文章编号:1672-3961(2007)05-0083-06

Fade statistics of selection diversity in distributed antenna systems

LI Zheng¹, WANG Xiao-dong², BU Zhi-yong³

(1. Department of Electronic Engineering, Naval Aeronautical Engineering Institute, Yantai 264001, China;
2. Department of Navigation and Communication, Naval Submarine Academy, Qingdao 266071, China;
3. Shanghai Research Center for Wireless Communications, Shanghai 200050, China)

Abstract: In the selection of combining distributed antenna systems, exact expressions for the average level crossing rate (LCR) and average fade duration (AFD) of the output signal envelope are derived. The diversity branches are assumed to be independent but non-identical composite fading channels. The results are valid for arbitrary diversity order and the amount of fading, and are obtained for Rayleigh-lognormal, Ricean-lognormal and Nakagami-lognormal composite fadings. Numerical results validate the derived expressions.

Key words: distributed antenna access system; composite fading channel; selection diversity; average level crossing rate; average fade duration

分布式天线系统中选择合并的衰落统计分析

李政¹, 王晓东², 卜智勇³

(1. 海军航空工程学院 电子工程系, 山东 烟台 264001; 2. 海军潜艇学院 航海观通系, 山东 青岛 266071;
3. 上海无线通信研究中心, 上海 200050)

摘要:对于采用选择合并方案的分布式天线系统,当各分集支路经受独立且不等同分布的复合衰落时,分析了系统合并输出包络的平均电平交叉率和平均衰落持续时间,得到这些二阶统计量的精确表达式.该方法对于任意分集支路数目下的 Rayleigh-lognormal, Ricean-lognormal 和 Nakagami-lognormal 三种复合衰落环境均是有效的.仿真结果验证了所得表达式的正确性.

关键词:分布式天线系统;复合衰落信道;选择分集;平均电平交叉率;平均衰落持续时间

中图分类号:TN911.2 文献标志码:A

0 Introduction

Fade statistics of the received signal envelope in terms of average LCR and AFD play important roles in the design of wireless communication systems and the analysis of its performance. For example, the average LCR and AFD provide the statistics of burst errors, which are of great important for the design of interleaver size and error-correcting codes^[1]. Closed form expressions for the average LCR and AFD have only been derived in small scale fading only models, characterized by Rayleigh^[2], Ricean^[3], Nakagami- m ^[4] distributions, etc. Tjhung presented LCR and AFD expressions for Rayleigh-lognormal (Suzuki) fading, Ricean-fading (RLN), and Nakagami-lognormal (NLN) composite fading channels^[5-6].

Received date: 2006-09-25

Foundation item: This work is partially supported by the China 863 Project (2005AA123510)

Biography: LI Zheng(1975-), male, Master, Lecturer, his research interests include electronic countermeasure and communication signal processing.

E-mail: wxd1005@sohu.com

Recently, distributed antenna systems (DASs), have captured the attention of many researchers owing to the power and capacity advantages of the DAS^[7]. Previous research on DAS have been focused on its gains due to shortened access-distance and inherent macroscopic diversity between distributed access ports. There exists, however, no study on the channel models of distributed access systems, especially on fading statistics analysis of diversity techniques in DAS, which are very important in the design of these systems.

The aim of this paper is to analyze and evaluate the LCR and AFD of SC, considering the Suzuki, RLN, and NLN fading models.

1 System model

In distributed antenna system, L widely spacing radio ports (RPs) are only used to transmit signals on the downlink and receive signals on the uplink and each RP is composed of an antenna and frequency-conversion device. All antennas are separately connected to the central unit (CU) by means of multiplexing technique. The signals associated with different connected remote antennas are processed using advanced signal processing techniques at CU. It is assumed that received signals suffer from flat fading, and the received signal at the i th RP is

$$z_i(t) = r_i(t) \cos(\omega_c t + \phi_i(t)) + n_i(t), \quad i = 1, \dots, L \quad (1)$$

where ω_c is carrier frequency; $n_i(t)$ is zero-mean AWGN process; $\phi_i(t)$ is the random phase; and $r_i(t)$ is the received signal envelope at any time t .

In DAS, due to the nature of largely separated RPs, $r_i(t)$ should encompass not only the small scale fading process $x_i(t)$ but also the lognormal shadowing process $s_i(t)$, that is $r_i(t) = x_i(t)s_i(t)$ with the JPDF $f_{r_i, x_i}(x_i, s_i)$ ^[5,6].

The PDF of r_i can be obtained by using the relation[8, Eq. (6-43)]

$$f_{r_i}(r_i) = \int_0^\infty f_{x_i, s_i}(r_i/s_i, s_i) \cdot (1/s_i) ds_i, \quad r_i \geq 0 \quad (2)$$

1.1 PDF and CDF of r_i

In the absence of a line-of-sight (LoS) component, r_i is Suzuki distributed^[9]; when there is a LoS component, r_i is RLN distributed^[3]; when statistical variations of $x_i(t)$ are distributed as the general Nakagami- m distribution, r_i is NLN distributed^[10]. Both RLN and NLN distributions cover the Suzuki distribution as a special case. Extending from the results of [6] and using the Gauss-Hermite quadrature[11, Eq. (25.4.46)], a new uniform expression of probability density function (PDF) for these composite fading distributions can be obtained as

$$f_{r_i}(r_i) = \sum_{l=1}^N \{\bar{\omega}_l f_l(r_i)/\sqrt{\pi}\}, \quad r_i \geq 0 \quad (3)$$

where N is the degree of the Hermite polynomial $H_N(t)$, $\bar{\omega}_l$ is the l th weight factor given by [11, Table 25.10], and $f_l(r_i)$ for Suzuki, RLN, and NLN models are, respectively

$$f_l(r_i) = \begin{cases} \frac{2r_i}{\Omega_i \eta_u^2} \exp\left(-\frac{r_i^2}{\Omega_i \eta_u^2}\right), & \text{Suzuki} \\ \frac{2(1+K_i)r_i}{\Omega_i \eta_u^2} \exp\left(-K_i - \frac{r_i^2(1+K_i)}{\Omega_i \eta_u^2}\right) I_0\left(\frac{2r_i}{\eta_u} \sqrt{\frac{K_i(1+K_i)}{\Omega_i}}\right), & \text{RLN} \\ \frac{2m_i^{m_i} r_i^{2m_i-1}}{\Omega_i^m \Gamma(m_i) \eta_u^{2m_i}} \exp\left(-\frac{m_i r_i^2}{\Omega_i \eta_u^2}\right), & m_i \geq \frac{1}{2} \end{cases} \quad \text{NLN}$$

where $\Omega_i = E[x_i^2]$, K_i and m_i are fading parameters of RLN and NLN, respectively; $I_0(\cdot)$ is the zero-order modified Bessel function of the first kind, $\Gamma(\cdot)$ is the Gamma function; $\eta_u = 10^{[(\sqrt{2}\sigma_i + \mu_i)/20]}$, t_l is the l th zero of $H_N(t)$, $\mu_i = E[20\lg(s_i)]$ denotes the area mean power of the signal received from the i th branch, and σ_i is the standard deviation of $20\lg(s_i)$, μ_i and σ_i are both in dB.

Integrating (3) with r_i , the CDF of r_i can be derived as

$$F_R(r_i) = \sum_{i=1}^N \left\{ [\bar{\omega}_i F_i(r_i)] / \sqrt{\pi} \right\} \quad (4)$$

where $F_i(r_i)$ for Suzuki, RLN, and NLN models are, respectively

$$F_i(r_i) = \begin{cases} 1 - \exp\left(-\frac{r_i^2}{\Omega_i \eta_u^2}\right), & \text{Suzuki} \\ 1 - Q_1\left(\sqrt{2K_i}, \frac{r_i}{\eta_u} \sqrt{\frac{2(1+K_i)}{\Omega_i}}\right), & \text{RLN} \\ P\left(m_i, \frac{m_i r_i^2}{\Omega_i \eta_u^2}\right), m_i \geq \frac{1}{2} & \text{NLN} \end{cases}$$

where $Q_1(a, b)$ is the Marcum's Q-function [3, Eq. (6.67)] and $P(a, b)$ is the incomplete Gamma function [11, Eq. (6.5.1)]. The definitions of other parameters are the same as (3).

1.2 JPDF of r_i and its time derivative

The JPDF of r_i and its time derivative r_i is required to derive the average LCR and AFD. This can be derived using the relation [3, Eq. (6.58)]

$$f_{R_i, R_i}(r_i, r_i) = \int_0^{\infty} \int_{-\infty}^{\infty} \frac{1}{y^2} f_{X_i, x_i}\left(\frac{x_i}{y}, \frac{t}{y} - \frac{y r_i}{y^2}\right) f_{S_i, s_i}(y, y) dy dy, r_i \geq 0, -\infty < r_i < \infty \quad (5)$$

where $f_{X_i, x_i}(x_i, x_i)$ is the JPDF of the small scale fading envelope and its time derivative^[12], $f_{S_i, s_i}(s_i, s_i)$ is the JPDF of the shadowing envelope and its time derivative^[3].

Extending from the results of reference [6] and using the Gauss-Hermite quadrature, a new uniform expression of the JPDF for these composite fading models can be derived as

$$f_{R_i, R_i}(r_i, r_i) = \frac{1}{\sqrt{\pi}} \sum_{i=1}^N \left\{ \bar{\omega}_i f_i(r_i) \left[\frac{1}{\sqrt{2\pi \zeta_u^2}} \exp\left(-\frac{r_i^2}{2\zeta_u^2}\right) \right] \right\} \quad (6)$$

where $\zeta_u^2 = (2\pi\sigma_e h\sigma_i r_i)^2 + b_i \eta_u^2$, $b = \ln(10)/20$, $f_i(r_i)$, σ_i , and η_u are the same as (3); b_i is given by^[14]

$$b_i = \begin{cases} (\pi f_m)^2 \Omega_i, & \text{Suzuki} \\ (\pi f_m)^2 \Omega_i / (K_i + 1), & \text{RLN} \\ (\pi f_m)^2 \Omega_i / m_i, & \text{NLN} \end{cases}$$

where f_m is the maximum Doppler frequency shift, Ω_i , K_i , and m_i are the same as (3); σ_e is related to f_c according to $\sigma_e = f_c / \sqrt{2\ln 2}$, where f_c is the 3 dB cutoff frequency of the power spectral density of colored Gaussian $v(t)$, which process can be used to generate the lognormal process by means of the nonlinear transform $s_i(t) = 10^{[(\sigma_e v(t) + \mu_i)/20]}$ [3, Sect. 6.1.2]. In general, f_c is in general much smaller than f_m . In order to simplify the notation, the symbol κ_e is introduced for the frequency ratio f_m/f_c , i.e., $f_c = f_m/\kappa_e$.

Equation (6) shows that the processes $r_i(t)$ and $r_i(t)$ are statistically dependent although the small scale fading processes $x_i(t)$ and $x_i(t)$ are statistically independent.

2 Average LCR and AFD of the SC output signal envelope

The average LCR and AFD of the SC output signal envelope, at given level, are given by [2, Eq. (1.3-32) and Eq. (1.3-41)]

$$N_R(\Re) = \int_0^{\infty} t f_{R\Re}(\Re, t) dt \quad (7)$$

$$\tau_R(\Re) = F_R(\Re) / N_R(\Re) \quad (8)$$

where $f_{R\Re}(r, t)$ is the JPDF of the SC output signal envelope r and its time derivative t , and $F_R(\Re)$ is the CDF of r at the specified level \Re .

A selection diversity combiner picks the input branch with the largest instantaneous signal-to-noise ratio.

Assuming the noise power of the input branches are the same, the SC output signal envelope r can be written as $r = \max(r_1, r_2, \dots, r_L)$, and its time derivative $\dot{r} = \dot{r}_i$ if $r_i = \max(r_1, \dots, r_L)$. Defining the event $\mathcal{A}_i = \{r_i = \max(r_1, \dots, r_L)\}$, then $\{\mathcal{A}_1, \mathcal{A}_2, \dots, \mathcal{A}_L\}$ forms a partition of probability space of r . Thus, the JCDF of r and \dot{r} can be expressed as a summation

$$F_{R\dot{R}}(r, \dot{r}) = \sum_{i=1}^L \Pr(R \leq r, \dot{R} \leq \dot{r}, \mathcal{A}_i) \quad (9)$$

where $\Pr(R \leq r, \dot{R} \leq \dot{r}, \mathcal{A}_i)$ is the probability of the event $\{R \leq r, \dot{R} \leq \dot{r}, \mathcal{A}_i\}$, which can be expressed as

$$\Pr(R \leq r, \dot{R} \leq \dot{r}, \mathcal{A}_i) = \Pr(R_i \leq r, \dot{R}_i \leq \dot{r}, \mathcal{A}_i) = \Pr(R_i \leq r, \dot{R}_i \leq \dot{r}, \{R_j \leq R_i\}_{j=1, \dots, L, j \neq i}) = \int_0^r \int_{-\infty}^{\dot{r}} \dots \int_0^{\dot{r}_i} f_{R_1, R_2, \dots, R_L}(\underbrace{r_1, r_2, \dots, r_L}_{\text{exclude } r_i}) dr_1 dr_2 \dots dr_L \quad (10)$$

Assuming the L composite fading branches to be mutually independent, i.e., $\{r_i, \dot{r}_i\}$ independent of $\{r_j, \dot{r}_j\}$, $\forall j \neq i$; and knowing that the composite fading process and its time derivative are statistically dependent, then (10) can be written as

$$\Pr(R \leq r, \dot{R} \leq \dot{r}, \mathcal{A}_i) = \int_0^r \int_{-\infty}^{\dot{r}} f_{R_i, \dot{R}_i}(r_i, \dot{r}_i) \prod_{j=1, j \neq i}^L F_{R_j}(r_j) dr_i d\dot{r}_i \quad (11)$$

Substituting (11) in (9) yield the JCDF of r and \dot{r} is

$$F_{R\dot{R}}(r, \dot{r}) = \sum_{i=1}^L \left[\int_0^r \int_{-\infty}^{\dot{r}} f_{R_i, \dot{R}_i}(r_i, \dot{r}_i) \prod_{j=1, j \neq i}^L F_{R_j}(r_j) dr_i d\dot{r}_i \right] \quad (12)$$

Differentiating (12) with respect to r and \dot{r} , the JPDF of r and \dot{r} for selection diversity is

$$f_{R\dot{R}}(r, \dot{r}) = \sum_{i=1}^L \left[f_{R_i, \dot{R}_i}(r, \dot{r}) \prod_{j=1, j \neq i}^L F_{R_j}(r_j) \right] \quad (13)$$

where $f_{R_i, \dot{R}_i}(r, \dot{r})$ is given by (6) and $F_{R_i}(r)$ is given by (4).

From (6), (13), and (7), the average LCR of the SC output signal envelope can be expressed as

$$N_R(\mathfrak{R}) = \sum_{i=1}^L \left[N_{R_i}(\mathfrak{R}) \prod_{j=1, j \neq i}^L \mathfrak{F}_{R_j}(\mathfrak{R}) \right] \quad (14)$$

where $N_{R_i}(\mathfrak{R}) \sum_{i=1}^N \left[(\bar{\omega}_i f_i(\mathfrak{R}) \sqrt{\xi_i^2/2}) / \pi \right]$ is the average LCR of the signal envelope of the i th diversity branch, $\bar{\omega}_i$ and $f_i(\mathfrak{R})$ are the same as (3), $\xi_i^2 = (2\pi\sigma_i h\sigma_i \mathfrak{R})^2 + b_i \eta_i^2$, the parameters included in ξ_i are given by (6); $F_{R_i}(\mathfrak{R})$ is the CDF of the signal envelope of the i th diversity branch at a specified level \mathfrak{R} given by (4).

By taking into account the independence assumption of r_i , $i = 1, \dots, L$, the CDF of the SC output signal envelope is

$$F_R(r) = \Pr(R_1 \leq r, \dots, R_L \leq r) = \prod_{i=1}^L F_{R_i}(r) \quad (15)$$

From (14), (15), and (8), the AFD of the SC output signal envelope can be expressed as

$$\tau_R(\mathfrak{R}) = \frac{1}{\sum_{i=1}^L (N_{R_i}(\mathfrak{R}) / F_{R_i}(\mathfrak{R}))} \quad (16)$$

where $N_{R_i}(\mathfrak{R})$ and $F_{R_i}(\mathfrak{R})$ are the same as (14).

Using (3), (4), (6), (14), and (16), the average LCR and AFD of the SC output Envelope in Suzuki, RLN, and NLN composite fading channels can be obtained. To the best of the author's knowledge, these results are new. For $\mu_i = \sigma_i = 0$, $\forall i = 1, 2, \dots, L$, the results we derived reduce to the expressions for the average LCR and AFD of SC output envelope in small scale fading only channel models, which are presented in [12, Eq.(17)-Eq.(19)].

3 Numerical results

The average LCR and AFD expressions presented above are computed and plotted in logarithmic scale against the combined received envelope in decibels. The simulation results are also plotted. In all figures, the markers correspond to the simulation points and the lines are the analytical curves.

Fig.1 and Fig.3 compare the average LCR (normalized by f_m) for SC with different diversity orders L and no-diversity case $L = 1$, for the Suzuki, NLN fading channels, and RLN fading channel. Fig.2 compares the normalized AFD for SC with different diversity orders L and no-diversity case $L = 1$ for the Suzuki, NLN fading channels. All simulation results are in excellent agreement with theoretical curves.

It can be observed from Fig.1 and Fig.3 that, for both fading conditions, as a consequence of the improvement of the output signal with the increase of the number of diversity orders, lower levels are crossed at lower rates whereas higher levels are crossed at higher rates. It also can be noted that the presence of a specular component ($K > 0$) or a decreasing of the amount of fading ($m > 1$) generally causes a lower LCR and hence, improves the performance of the communication systems. Fig.2 shows that, for both fading conditions, as a consequence of the improvement of the output signal with the increase of the number of diversity orders, the signal of SC output has less time in fading.

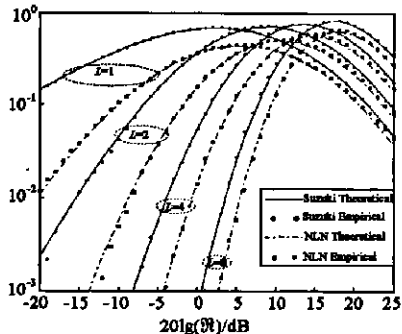


Fig.1 Normalized average LCR for SC with diversity orders L for the Suzuki and NLN fading channels, with $\mu_i = 5$, $\sigma_i = 8$, $\Omega_i = 2$, $m_i = 2$, $\kappa_e = 10$

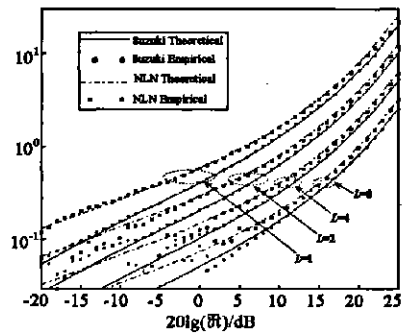


Fig.2 Normalized AFD for SC with diversity orders L for the Suzuki and NLN fading channels, with $\mu_i = 5$, $\sigma_i = 8$, $\Omega_i = 2$, $m_i = 2$, $\kappa_e = 10$.

In order to compare the LCRs and AFDs of unbalanced diversity branches to those of balanced diversity branches, the unbalanced for Suzuki channels and unbalanced amount of fading for NLN channels were analyzed and simulated as shown in Figure 4.

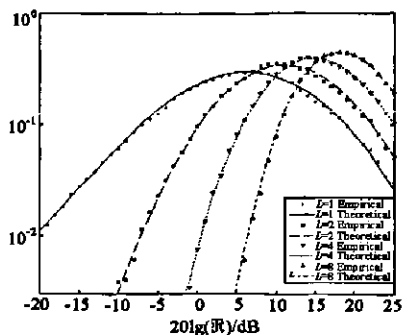


Fig.3 Normalized average LCR for SC with diversity orders L for the RLN fading channels, with $\mu_i = 5$, $\sigma_i = 8$, $\Omega_i = 2$, $K_i = 4$, $\kappa_e = 10$

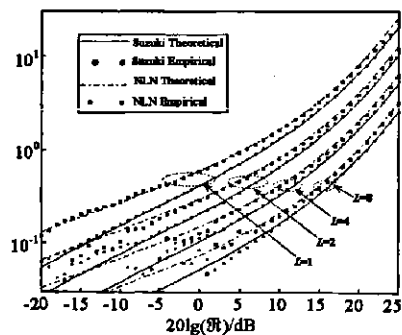


Fig.4 Normalized average LCR for SC with diversity orders L for the Suzuki and NLN fading channels. Bal. means the balanced channels and unbal. means the unbalanced channels

In Figure 4, a situation with parameters $\mu = [5, 5], \sigma = [8, 8], \Omega = [2, 2]$ as balanced benchmark for the Suzuki unbalanced channel model with $\sigma = [4, 12]$, and set a situation with parameters $\mu = [5, 5], \sigma = [8, 8], \Omega = [2, 2], m = [1.5, 1.5]$ as balanced benchmark for the NLN unbalanced channel with $m = [0.5, 2.5]$ was set. It can be seen that the average LCR of unbalanced diversity signals have a higher crossing rate than balanced signals at lower levels, and the average LCRs are about the same at higher levels. Figure 4 also shows that unbalanced shadowings have a smaller effect on the average LCR than an unbalanced amount of fading of small scale fading only.

4 Conclusion

In this paper, exact analytical expressions for the average level crossing rate and average fade duration of SC diversity with independent but non-identical composite Suzuki, Ricean-lognormal, and Nakagami-lognormal fading channels in distributed wireless access systems were derived and validated by simulation. The material presented can be used in analyzing error correcting schemes for burst error channels and determine the minimum duration outages of composite fading channels.

References:

- [1] TSAI S, SCHMIED P S. Interleaving and error-burst distribution[J]. IEEE Trans Commun, 1972, 20(3):291-296.
- [2] JAKES W C. Microwave mobile communications[M]. New York: IEEE Press, 1994.
- [3] MATTHIAS P. Mobile fading channels[M]. West Sussex: John Wiley & Sons, 2002.
- [4] YACOUB M D, BAUTISTA J E, GUEDES L G. On higher order statistics of the Nakagami-m distribution[J]. IEEE Trans Veh Technol, 1999, 48(3):790-794.
- [5] TJHUNG T T, CHAI C C. Fade statistics in microcellular mobile radio channels with shadowing[J]. IEEE, 1998: 1645-1649.
- [6] TJHUNG T T, CHAI C C. Fade statistics in Nakagami-lognormal channels[J]. IEEE Trans Commun, 1999, 47(12):1769-1772.
- [7] YU X H, CHEN G A, CHEN M, et al. Toward beyond 3G: the FuTURE project in China[J]. IEEE Commun Mag, 2005, 43(1):70-75.
- [8] PAPOILIS A. Probability, random variables, and stochastic processes[M]. 3rd ed. New York: McGraw-Hill, 1991.
- [9] SUZUKI H. A statistical model for urban radio propagation[J]. IEEE Trans Commun, 1977, 25(7):673-680.
- [10] STÜBER G L. Principles of mobile communication[M]. 2nd ed. New York: Kluwer Academic Publishers, 2002.
- [11] ABRAMOWITZ M, STEGUN I A. Handbook of mathematical functions with formulas, graphs and mathematical tables[M]. 9th ed. New York: Dover, 1970.
- [12] DONG X F, BEAULIEU N C. Average level crossing rate and average fade duration of selection diversity[J]. IEEE Commun Let, 2001, 5(10):396-398.

(编辑:胡春霞)

如何学习天线设计

天线设计理论晦涩高深，让许多工程师望而却步，然而实际工程或实际工作中在设计天线时却很少用到这些高深晦涩的理论。实际上，我们只需要懂得最基本的天线和射频基础知识，借助于 HFSS、CST 软件或者测试仪器就可以设计出工作性能良好的各类天线。

易迪拓培训(www.edatop.com)专注于微波射频和天线设计人才的培养，推出了一系列天线设计培训视频课程。我们的视频培训课程，化繁为简，直观易学，可以帮助您快速学习掌握天线设计的真谛，让天线设计不再难…



HFSS 天线设计培训课程套装

套装包含 6 门视频课程和 1 本图书，课程从基础讲起，内容由浅入深，理论介绍和实际操作讲解相结合，全面系统的讲解了 HFSS 天线设计的全过程。是国内最全面、最专业的 HFSS 天线设计课程，可以帮助你快速学习掌握如何使用 HFSS 软件进行天线设计，让天线设计不再难…

课程网址: <http://www.edatop.com/peixun/hfss/122.html>

CST 天线设计视频培训课程套装

套装包含 5 门视频培训课程，由经验丰富的专家授课，旨在帮助您从零开始，全面系统地学习掌握 CST 微波工作室的功能应用和使用 CST 微波工作室进行天线设计实际过程和具体操作。视频课程，边操作边讲解，直观易学；购买套装同时赠送 3 个月在线答疑，帮您解答学习中遇到的问题，让您学习无忧。

详情浏览: <http://www.edatop.com/peixun/cst/127.html>



13.56MHz NFC/RFID 线圈天线设计培训课程套装

套装包含 4 门视频培训课程，培训将 13.56MHz 线圈天线设计原理和仿真设计实践相结合，全面系统地讲解了 13.56MHz 线圈天线的工作原理、设计方法、设计考量以及使用 HFSS 和 CST 仿真分析线圈天线的具体操作，同时还介绍了 13.56MHz 线圈天线匹配电路的设计和调试。通过该套课程的学习，可以帮助您快速学习掌握 13.56MHz 线圈天线及其匹配电路的原理、设计和调试…

详情浏览: <http://www.edatop.com/peixun/antenna/116.html>



关于易迪拓培训:

易迪拓培训(www.edatop.com)由数名来自于研发第一线的资深工程师发起成立,一直致力于专注于微波、射频、天线设计研发人才的培养;后于 2006 年整合合并微波 EDA 网(www.mweda.com),现已发展成为国内最大的微波射频和天线设计人才培养基地,成功推出多套微波射频以及天线设计经典培训课程和 **ADS**、**HFSS** 等专业软件使用培训课程,广受客户好评;并先后与人民邮电出版社、电子工业出版社合作出版了多本专业图书,帮助数万名工程师提升了专业技术能力。客户遍布中兴通讯、研通高频、埃威航电、国人通信等多家国内知名公司,以及台湾工业技术研究院、永业科技、全一电子等多家台湾地区企业。

我们的课程优势:

- ※ 成立于 2004 年, 10 多年丰富的行业经验
- ※ 一直专注于微波射频和天线设计工程师的培养, 更了解该行业对人才的要求
- ※ 视频课程、既能达到了现场培训的效果, 又能免除您舟车劳顿的辛苦, 学习工作两不误
- ※ 经验丰富的一线资深工程师主讲, 结合实际工程案例, 直观、实用、易学

联系我们:

- ※ 易迪拓培训官网: <http://www.edatop.com>
- ※ 微波 EDA 网: <http://www.mweda.com>
- ※ 官方淘宝店: <http://shop36920890.taobao.com>